Attention, Perception, & Psychophysics
2010, 72 (5), 1350-1366
doi:10.3758/APP.72.5.1350

Virtual and drawing structures for the Müller-Lyer illusions

Gordon M. Redding and David W. Vinson
Illinois State University, Normal, Illinois

This research assessed the relative contribution of 3-D virtual structure that generated the stimulus drawings (scene-based and picture-based theories) and 2-D structure of the drawings (object-based theories). Virtual structures were right-angle convex and concave corners in front of and behind the picture plane, respectively. Virtual corner size was manipulated directly (Experiment 1) and indirectly by manipulating drawing station point distance (Experiments 2 and 3), corner depth (Experiment 4), and corner distance from the picture plane (Experiments 5 and 6). Experiments 2 and 4 held the size of the projected corner edge (interior target line) constant, causing virtual corner size to vary, whereas Experiments 3, 4, 5, and 6 held size of the virtual corners constant, causing size of the projected corner edge or interior target line to vary. Subjects reproduced the length of the projected corner edge (interior target line). The illusions (difference between reproduced size of the projected corner edge and T-junction control) were generally well fit by the weighted sum of virtual corner size and size of the projected corner edge, but the projected distance between boundary line terminations (intertip distance) appeared as an additional contributing factor in Experiments 5 and 6. The implications of this methodological approach are discussed for theories of the illusions.

A common assumption is that visual illusions arise from multiple sources (Coren & Girgus, 1978a, 1978b). If this assumption is correct, the appropriate research question is: How much of an illusion can be attributed to each source, and under what conditions? Another assumption is that illusions arise "when the visual system is asked to perform some task to which it is ill adapted" (Morgan, Hole, & Glennerster, 1990, p. 1800), "when information well suited for one kind of task is employed in tasks for which it is not well suited" (Redding & Hawley, 1993, p. 827). The present research was guided by these assumptions. Three major kinds of theories, which meet the second assumption, were contrasted to evaluate their relative contributions to the Müller-Lyer illusions. First, we critique the theories to clearly identify the assumed underlying sources; then, under the first assumption, we propose a model of how these processes may combine to produce the total illusions. Finally, we report a series of experimental tests of this combinatorial model.

Theories of the Müller-Lyer Illusions

Scene-based theories (Gillam, 1978, 1980, 1998; Gregory, 1963, 1965, 1967, 1968, 1974; Gregory & Harris, 1975) assume that visual illusions reflect the operation of processes that normally serve to enable development of a scene representation from the natural perspective information present in the 2-D retinal image. When processes evolved for the analysis of natural perspective are applied to the linear perspective information present in a 2-D drawing, they produce consistent interpretation biases that, although appropriate for natural perspective, are inappropriate for linear perspective. Visual illusions are the consequences of such biases.[1]

For example, Gillam (1978, 1980, 1998) has proposed a scene-based theory in the spirit of Gregory's *inappropriate primary constancy scaling* hypothesis.[2] She has interpreted primary constancy scaling in terms of Gibson's (1966) direct size scaling process, proposing an orthogonalization process (see also Mountjoy, 1966) in natural perspective analysis that works to minimize acute and obtuse angles in the 2-D retinal image to recover the more likely right angles in a scene (Perkins, 1972, 1973; Shepard & Smith, 1971, reported in Shepard, 1981). "Orthogonalization can be thought of as a form of primary shape scaling associated with size scaling" (Gillam, 1978, p. 61). Lines forming acute or obtuse angles tend to be rotated about pivot points located along the line to produce more of a right-angle perception. When inappropriately applied to linear perspective drawings, orthogonalization tends to reduce the perceived length of lines forming acute angles and increase the perceived length of lines forming obtuse angles. Gillam (1978) has noted that such a theory can account for most of the basic facts about the Müller-Lyer illusion.[3]

Picture-based theories (Kubovy, 1986; Perkins, 1972, 1973; Pirenne, 1970; Shepard, 1981, 1990; Yang & Kubovy, 1999) assume that visual illusions reflect the operation of processes that normally serve to enable de-

G. M. Redding, gredding@ilstu.edu

velopment of a 3-D representation from the linear perspective information present in 2-D pictures—that is, the perception of pictures.[4] When processes evolved for the analysis of linear perspective are applied to line drawings with minimal perspective information, they produce consistent interpretation biases that, although appropriate for full linear perspective drawings, are inappropriate for minimal perspective line drawings. Visual illusions are the consequence of such biases.

For example, Farber and Rosinski (1978; Rosinski & Farber, 1980) proposed that picture perception proceeds by a process of recovering the station point from which the picture was drawn. Such an inverse perspective process tends to produce perception of the original size of the depicted object, which contrasts with the drawn size. When station point recovery is applied to minimal perspective line drawings like the Müller-Lyer figures, size perception is reduced for the arrow-junction figure, which depicts a smaller object, and enlarged for the fork-junction figure, which depicts a larger object.

Object-based theories (Coren & Girgus, 1978a, 1978b; Girgus & Coren, 1982; Morgan et al., 1990; Redding, Winson, & Temple, 1993; see also Jordan & English, 1989; Jordan & Haleblian, 1988; Jordan & Schiano, 1986; Jordan & Uhlarik, 1985, 1986) assume that geometric illusions reflect the information processing that normally serves to enable the development of 3-D object representations from the 2-D pattern of lines projected onto the retina. When judgments of selected object attributes are made on the basis of a grouping of lines for object representation, those judgments are biased by the average attribute value (Pressey, 1970, 1972, 1974; Pressey & Pressey, 1992). Processes adapted for object representation may bias processes directed toward distinguishing the parts that compose an object. Visual illusions are the consequences of such biases.

For example, Pressey (1970, 1972, 1974) proposed that perceptual representation proceeds by a process of averaging ("assimilation" toward the mean) size attributes of a candidate stimulus array. Such an averaging process produces object dimensions that contrast with that of the object parts. When object representation processes are applied to stimulus arrays like the Müller-Lyer figures, size perception of the central line is reduced for the arrow-junction figure because the average object size is less, and enlarged for the fork-junction figure because the average object size is larger.

The first two kinds of theories assume an implicit or *virtual* perspective source structure for line drawings that produce illusions. Scene-based theories propose that judgment of line drawings is biased by the virtual structure produced by natural perspective interpretation. Picture-based theories propose that judgment of line drawings is biased by the virtual structure produced by linear perspective interpretation. Object-based theories, while assuming some perspective source structure for objects, propose that judgment of a target line in a drawing is biased by primitive grouping of the drawn lines; therefore, such theories assume that illusions arise from a drawing biases among elements of the 2-D drawing produced in the early stages of object processing (cf. Marr, 1982). The three kinds of theories are not mutually exclusive.

The theories arguably depend on information available at different levels of perceptual processing. In object-based theories, illusions arise from low-level processing of the segmented stimulus array to form groupings of elements. In scene-based theories, illusions arise from intermediate-level processing to form a 3-D volumetric representation. In picture-based theories, illusions arise in high-level processing, where the rules of linear perspective are applied to an object representation. The suggested biases occur at successive stages of perceptual processing, where the input of a later stage of processing is the result of the preceding stage. If this view of perceptual processing is correct, the total illusion should be the sum all of these successive biases. We suppose an additive model, where the total illusion is the sum of independent contributions at successive levels of perceptual processing. In the present research, we manipulated the source structures assumed by each kind of theory to determine whether the resultant illusions combine in an additive manner. In general, an alternative hypothesis is that successive stages of processing are not independent, and that, depending on the output of an earlier stage, processing at a later stage will be different. A number of more complicated alternatives to an additive model would have to be investigated, should a simple additive model fail to fit the data.

Source Structures

The present research investigated possible virtual structures for the Müller-Lyer illusions (Müller-Lyer, 1889/1981). We begin with the known constraints on possible virtual structure. First, in the absence of other visible junctions, arrow and fork junctions are interpretable as boundary junctions that occlude other structures and are constrained to represent convex and concave corners, respectively (Redding & Hawley, 1993). Second, both figures are assumed to depict dihedral angles formed by two planes (Rosinski & Farber, 1980), intersecting at right angles (Perkins, 1972, 1973; Shepard & Smith, 1971, reported in Shepard, 1981).

We further make the assumption that the virtual convex corner is located in front of the picture plane, and that the virtual concave corner is located behind the picture plane. This assumption is based on the empirical fact that the arrow-junction drawing (virtual convex corner projection) and the fork-junction drawing (virtual concave corner projection) usually elicit smaller and larger size judgments, respectively, than do control stimuli, which are arguably not influenced by natural or linear perspective bias or the averaging bias of object representation. Assuming that the illusions arise from virtual structure bias, the only way in which this empirical regularity could occur is if virtual convex and concave corners are located in front of and behind the picture plane, respectively. Finally, we initially make the simplifying assumption that the boundary lines terminate in the picture plane (but see Experiments 5 and 6).

Therefore, the hypothesized linear perspective virtual structures, illustrated in Figure 1, are convex and concave right-angle corners located in front of and behind the picture plane, respectively, drawn as viewed from the station point. Hypothetical natural perspective virtual structures, also illustrated in Figure 1, are the same corners with the same relative position in space, but viewed from the more distant vantage point (40 cm) used in the present experiments. It turns out that the rules of perspective are such that drawings are always scaled down from the potential real size of the depicted object; that is, the drawing station point distance must be very short for the drawing to be of a manageable size. Consequently, picture perception necessarily involves some process that recognizes the original station point that produced the drawing, and scene perception necessarily involves some process that recognizes the impossibility of such extreme angles.

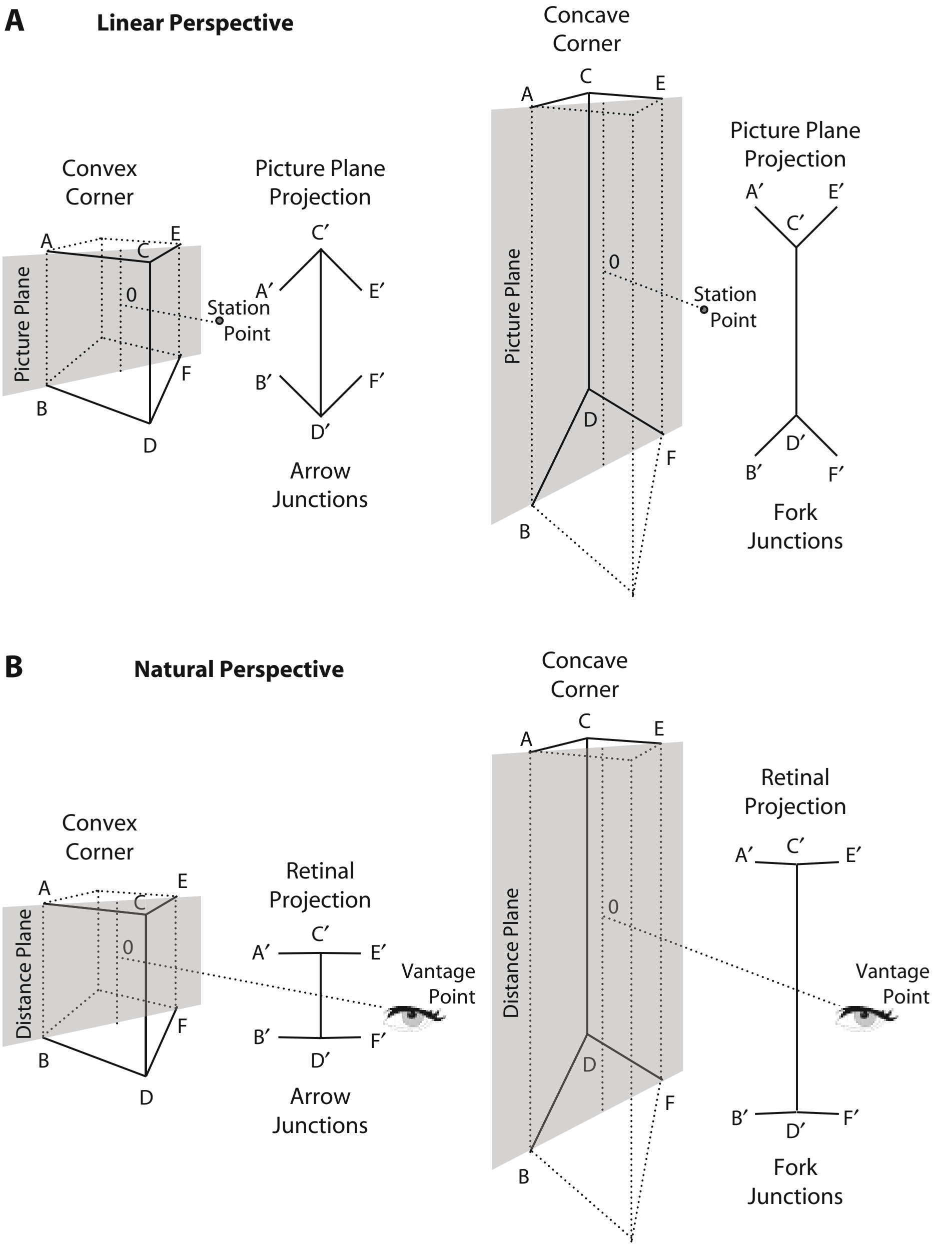

Figure 1. Virtual structure: Linear perspective views are given for convex and concave corners in front of and behind the picture plane that project to produce arrow and fork junctions, respectively. The illustrated station points are the positions of the artist's eye when the picture plane projections were constructed. Natural perspective is also illustrated for the same virtual corners viewed from the more distant vantage point (40 cm) from which subjects in the present experiments viewed the stimulus arrays.

With virtual structures so specified, the operations in picture-based and scene-based theories can be more clearly identified. When the picture plane projections produced by linear perspective are presented, picture-based theory assumes that the 3-D virtual structure that produced the stimulus is recovered and biases perception of the 2-D drawing: A primary process is station point recovery. On the other hand, the linear perspective drawings, when considered as retinal images in natural perspective, represent corners flattened in depth. The scene-based theory assumption of the retinal projection that would be produced by a full right-angle corner biases perception of the 2-D drawing; a primary process is rotation of angled lines toward the retinal image of a full right-angle corner (i.e., orthogonalization).

Given such constraints, virtual structure can be manipulated, and quantitative predictions can be made about size perception of the Müller-Lyer drawings. Importantly, because stimulus arrays are constrained by virtual structure, prediction from virtual structure can be contrasted with prediction from attribute averaging of the drawn structure.[5] Assuming that the illusions are multiply determined (Coren & Girgus, 1978a, 1978b), we tested the simple hypothesis that virtual and drawn structures combine additivity to produce the illusions.

Experiment 1 manipulated virtual corner size directly to assess the relative contribution to the illusions of this factor and the projected size of the corner edge: Note that projected size necessarily covaried with virtual size. Experiment 2 varied corner sizes indirectly and held projected size constant by manipulating the distance of the station point from which the drawings were made. Experiment 3 also manipulated the station point, but with corner size constant and projected size varying. Experiment 4 manipulated corner depth, holding corner size constant and varying projective size. Experiment 5 compared virtual and drawing components by manipulating corner distance from the picture plane, with virtual size constant and projected size varying. Experiment 6 replicated Experiment 5 and established generalization of results for different viewing times. These last two experiments enabled comparison of the relative contribution of virtual (picture-based or scene-based theory) and drawing average factors (object-based theory) to the illusions. Illusions were predicted to be the weighted sum of contributions from virtual sources and drawing sources and goodness of fit to prediction was assessed.

GENERAL METHOD

Nomenclature

The lines produced by 2-D projection of dihedral planes intersecting at right angles (3-D corners) can be partitioned into boundary lines and interior lines (Redding & Hawley, 1993; Waltz, 1975). Boundary lines occur when one plane occludes another and the two regions in the projection separated by a boundary line do not abut along the boundary line. Interior lines occur where the two planes join to form an edge and in projection the two separated regions abut one another. Such interior lines can be further partitioned into concave and convex edges. Corner vertices project as line junctions.

For example, in Figure 1, planes ACDB and CEFD join at right angles to form convex or concave edges, which project as interior line C′D′. Boundary lines A′C′, B′D′, C′E′, and D′F′ are projections of occluding edges AC, BD, CE, and DF, respectively. Line junctions A′C′E′ and B′D′F′ are the projections of corner vertices ACE and BDF, respectively. When corner edges are in front of and behind the picture plane they project as arrow junctions and fork junctions, respectively.

Subjects

Subjects were students at Illinois State University who volunteered in return for extra credit in their psychology courses. All subjects had self-reported normal vision or corrected-to-normal vision. All subjects were treated in accordance with the Ethical Principles of Psychologists and Code of Conduct (American Psychological Association, 1992).

Stimulus Generation

Stimuli were constructed as PICT documents using a graphics application (Aldus Super Paint 3.5) from point coordinates provided by a spreadsheet application (Microsoft Excel) that implemented algebraic point projection equations (Sedgwick, 1980). The point projection, drawing, and inverse equations are illustrated in Figure 2.

The Müller-Lyer figures are specified by the 2-D coordinates of six points (see Figure 1) marking the four terminations of the boundary lines (A′, B′, E′, F′) and the two junctions of boundary lines with the interior line (C′, D′). These 2-D coordinates for a 3-D corner with known structure and position relative to the station point and picture plane are given by solving the point projection equations in Figure 2 for the terminations of the four boundary edges and for the two three-faced vertices. Trigonometric functions were used to determine angles and distances. The drawing equation in Figure 2 gives the size of the virtual corner edge (V) projected as the interior target line of a drawing (P) and the inverse equation expresses drawings in terms of the virtual structure.

In general, unless otherwise noted, the right-angle virtual convex and concave corners were 0.8 cm deep (D) with boundary lines terminating in the picture planed and drawn from a station point (d) of 1.6 cm. Control stimuli were the length of the corresponding arrow or fork-junction stimulus interior target line, but stopped by a T junction half the length of the target line, forming a horizontal H-shaped figure. The precision of the drawings was ± 0.4 mm (one screen pixel) and $\pm 1°$.

Procedure

Each subject was seated, head constrained by a chin–forehead rest, with eyes 40 cm from the Apple 14-in. color monitor screen (640×480 resolution); the line of sight was perpendicular to the screen at a point 5 cm above the center of the screen. All stimulus lines were 1 screen pixel (0.4 mm) in width. A computer mouse was on the table in front of the subject for response. After onscreen instructions were read and questions answered, the experiment was initiated by a mouse click with the screen arrow cursor anywhere on the screen.

Each trial began with the appearance of a small box (0.5 cm square) centered on the screen. Subjects placed the screen arrow cursor inside the box, clicked the mouse, and the stimulus screen immediately appeared after the screen refresh delay (67 Hz). The stimulus array consisted of the centrally located box, now with a response line (8 cm) extending downward from the box, and a vertically oriented stimulus centered on a point 5.0 cm above the box. Subjects were instructed to place the tip of the arrow cursor on the response line, such that the distance from the cursor tip to the box matched the length of the stimulus. After positioning the cursor to reproduce the stimulus length, the subject clicked the mouse, and after an intertrial interval of 0.5 sec, the box alone reappeared to begin the next trial.

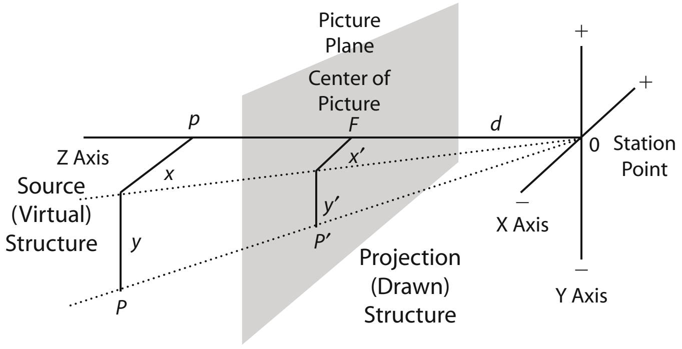

Point Projection of P to P'

$$x' = x(d/z)$$
$$y' = y(d/z)$$
$$z' = d$$

Projection (drawing) and Inverse Equations

$$P = V\ \frac{d}{d \pm D}$$
$$V = P\ \frac{d \pm D}{d}$$

P is the projected size for virtual corner size V
from station point d with corner depth D
($+$ for concave corners and $-$ for convex)

Figure 2. Coordinate system for linear perspective, together with point projection equations and drawing equations. (Adapted from Sedgwick, 1980; see also Freeman, 1986.)

Subjects received five randomized blocks of nine trials. The first block of trials was for practice and consisted of nine plain line stimuli without junctions to accustom the subject to reproducing the stimulus length. Otherwise for the subject, these practice stimuli were not distinguished in any way from the following experimental blocks.

Following the practice block, subjects received four random blocks of nine stimuli that included experimental stimuli with junctions, corresponding end-stopped control stimuli, and plain line filler stimuli without junctions. These filler stimuli were included to encourage a range of reproduction response and to reemphasize reproduction of the stimulus length, exclusive of junctions.

A Power Macintosh 7200 computer running the PsyScope (version 1.2.4 PPC) application (Cohen, MacWhinney, Flatt, & Provost, 1993) controlled the entire experiment. The computer, keyboard, and primary monitor were located at the opposite end of the table from the subject. Subjects saw only the secondary monitor on which the stimuli were presented.

Design

A mixed design was used in all experiments. Subjects were assigned in a pseudorandom fashion to levels of the manipulated virtual corner structure (and viewing time in Experiment 6), such that each level was approximately equally represented at any point in data collection. The within-subjects factors were stimulus (experimental and matching controls) and trial blocks. The trial-blocks factor was a replication variable for increased reliability and not analyzed.

Data Analysis and Hypotheses

The mouse click coordinates in screen pixels were converted to metric distance (25.6 pixels/cm) along the response line and these metric measures were submitted to analysis. Metric measures can be converted to visual angle measurements by the constant multiplier 1.43 because the viewing distance was constant (40 cm).

Before analysis, the reproduced size data were first normalized to the real value of the control stimuli to remove any judgmental bias not due to the junctions; that is, the signed difference between reproduced size and actual size of each control stimulus was subtracted from the reproduced size of both control and corresponding experimental stimuli. This adjustment to control values is necessary to obtain clean estimates of virtual and drawing factor contributions to reproduced size; but of course, such normalization does not affect illusion scores.

For Experiments 1 through 4, the reproduced size data were hypothesized to fit the following weighted equation, assessing the contributions of virtual and drawing structures to size judgments:

$$R = \omega_v V + \omega_p P, \qquad \text{(Hypothesis 1)}$$

where R is reproduced size, ω_v is the weighting given to virtual structure V, and ω_p is the weighting given to drawing structure P.

The virtual structure (V) is the size of the virtual corner edge, and the drawing structure (P) is the projected size of the corner edge as the interior target line. Expressed in terms of projection equations (see Figure 2), Hypothesis 1 becomes

$$R = \omega_v \left(P \frac{d \pm D}{d}\right) + \omega_p \left(V \frac{d}{d \pm D}\right), \qquad (1)$$

where d is the station point distance from the picture plane, and D is the virtual structure distance in depth from the picture plane ($-$ for structures in front of the picture plane, and $+$ for structures behind the picture plane).

Independent variables were virtual corner size, station point distance, and virtual corner depth. Either virtual size or drawing size was held constant in any given experiment, and Equation 1 was expressed solely in terms of the constant. For example, if drawing size P is constant, Equation 1 becomes:

$$R = \omega_v \left(P \frac{d \pm D}{d} \right) + \omega_p \left(P \frac{d \pm D}{d} \frac{d}{d \pm D} \right)$$
$$= \omega_v \left(P \frac{d \pm D}{d} \right) + \omega_p P.$$

Illusion scores were calculated by finding the reproduced size difference between an experimental stimulus and the corresponding control stimulus in the same block of trials. The average absolute (unsigned) values of these illusion scores were submitted to analysis. Illusion scores were evaluated in terms of virtual and drawing contributions with predicted fits to the following equations for the arrow-junction illusion (A, projection of a convex corner) and for the fork-junction illusions (F, projection of a concave corner):

$$I_A = C - R = C - \omega_v V - \omega_p P \tag{2}$$

and

$$I_F = R - C = \omega_v V + \omega_p P - C, \tag{3}$$

where C is the value of the size of the corresponding control stimulus.

Note that the drawing factor P is the target line, which has the same value as C, and when the sum of weights is constrained to equal 1, such that they represent proportional contributions, the equations reduce to

$$I_A = C - R = P - \omega_v V - (1 - \omega_v) P = \omega_v (C - V) \tag{4}$$

and

$$I_F = R - C = \omega_v V + (1 - \omega_v) P - P = \omega_v (V - C). \tag{5}$$

For the first three experiments, size of the virtual corner (V) and projected distance between boundary line terminations (I) were the same value, because boundary lines terminated in the picture plane, marking off the virtual corner size. Experiment 4 controlled for this confound by holding this second drawing factor (I) constant. Experiments 5 and 6 manipulated the distance of the visual corner from the picture plane, causing virtual size and this second drawing factor (I) to vary at different rates. For these experiments, the additional hypotheses were

$$R = \omega_I I + \omega_p P \tag{Hypothesis 2}$$

and

$$R = \omega_v V + \omega_I I + \omega_p P, \tag{Hypothesis 3}$$

where R is reproduced size, ω_v is the weighting given to virtual structure V, ω_p is the weighting given to drawing structure P, and ω_I is the weighting given to drawing structure I.

The second drawing structure factor (I) was the projected size of the distance between boundary line terminations (inter "wing" tip distance). Expressed in terms of projection equations, Hypotheses 2 and 3 become

$$R = \omega_I \left(V \frac{d}{d \pm (D - E)} \right) + \omega_p \left(V \frac{d}{d \pm D} \right) \tag{6}$$

and

$$R = \omega_v \left(P \frac{d \pm D}{d} \right) + \omega_I \left(V \frac{d}{d \pm (D - E)} \right)$$
$$+ \omega_p \left(V \frac{d}{d \pm D} \right), \tag{7}$$

where d is the station point distance from the picture plane, D is the virtual structure distance in depth from the picture plane ($-$ for structures in front of the picture plane, $+$ for structures behind the picture plane), and E is the constant corner depth.

For Hypotheses 2 and 3, illusion score Equations 2 and 3 become

$$I_A = C - R = C - \omega_I I - \omega_p P, \tag{8}$$

$$I_F = R - C = \omega_I I + \omega_p P - C, \tag{9}$$

$$I_A = C - R = C - \omega_v V - \omega_I I - \omega_p P, \tag{10}$$

and

$$I_F = R - C = \omega_v V + \omega_I I - C + \omega_p P. \tag{11}$$

EXPERIMENT 1
Virtual Corner Size

Perhaps the most obvious virtual factor is corner size. However, it should be noted that there are strict limits on virtual corner size that will produce manageably sized stimuli, as well as fall within the dioptic power of the human eye (Gregory & Harris, 1975; Warren & Bashford, 1977). For the first experiment, virtual corner size was manipulated within these limits. Note carefully that such direct manipulation of corner size necessarily means that the projected size of the corner edge or interior target line also varies, but at a different rate than virtual size.

Method

Virtual corner size was manipulated; projected size of the corner edge or interior target line also varied. Levels of corner size were 0.8, 1.2, 1.6, 2.0, 2.4, and 2.8 cm, producing interior target line sizes of 1.6, 2.4, 3.2, 4.0, 4.8, and 5.6 cm, respectively for convex corner drawings and 0.5, 0.8, 1.1, 1.3, 1.6, and 1.9 cm for concave corner drawings, respectively. These stimuli are illustrated in Figure 3. Groups of

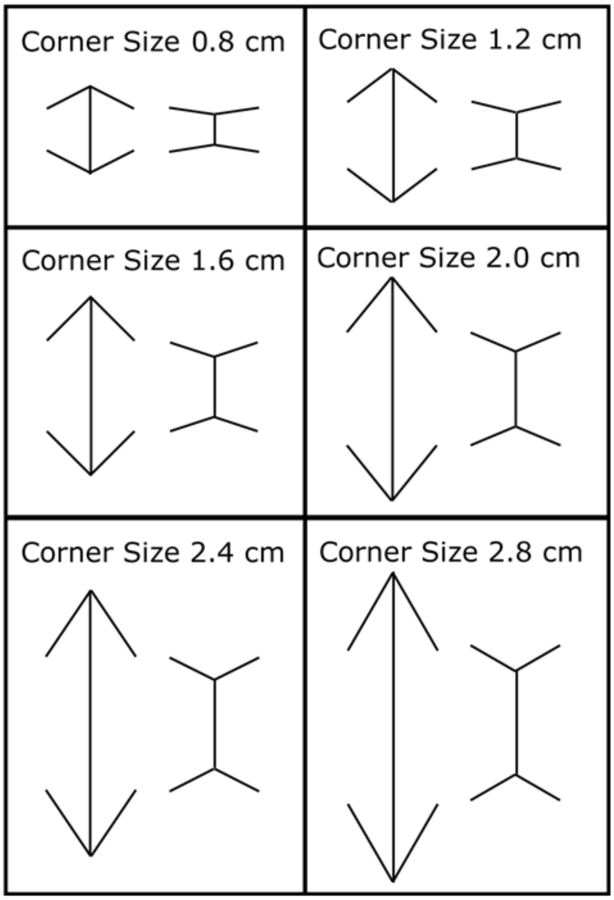

Figure 3. Experiment 1 stimuli as a function of virtual corner size.

subjects assigned to increasing levels of corner size numbered 24, 25, 51, 48, 25, and 25, respectively, for a total of 198 subjects.

Other drawing characteristics were, in order of increasing corner size for convex and concave corner drawings, respectively: interior angles of 63º, 53º, 45º, 39º, 34º, and 30º, and 99º, 104º, 108º, 113º, 117º, and 120º; projected boundary line lengths were 0.9, 1.0, 1.1, 1.3, 1.4, and 1.6 cm, and 0.8, 0.8, 0.8, 0.9, 0.9, and 0.9 cm; projected distances between boundary line terminations were the same as corner size; projected maximal width was constant at 1.6 cm.

The nine practice stimuli were, in order of increasing corner size: 0.3, 0.4, 0.5, 0.8, 1.1, 1.3, 1.6, 1.7, and 1.9 cm; 0.4, 0.6, 0.8, 1.2, 1.6, 2.0, 2.4, 2.6, and 2.8 cm; 0.5, 0.8, 1.1, 1.6, 2.1, 2.7, 3.2, 3.5, and 3.7 cm; 0.7, 1.0, 1.3, 2.0, 2.7, 3.3, 4.0, 4.3, and 4.7 cm; 0.8, 1.2, 1.6, 2.4, 3.2, 4.0, 4.8, 5.2, and 5.6 cm; and 0.9, 1.4, 1.9, 2.8, 3.7, 4.7, 5.6, 6.1, and 6.5 cm. The five filler stimuli were the same as the middle five of each set of nine practice stimuli. The two control stimuli were the projective size of the target line in the two experimental stimuli, but stopped by T junctions (see the General Method section).

Results

Normalization of the data to control values produced, on average, an addition of 0.01 cm ± 0.06 *SEM*, indicating a small tendency toward underestimation. Normalized reproduced size data for both corners were well fit ($R^2 = .99$) by Equation 1 (see the General Method section), with the sum virtual and drawing weights constrained to equal 1. Therefore, the contribution of virtual size to the illusions was assessed using Equations 4 and 5, as illustrated in Figure 4. As can be seen, taking the difference between experimental and variable control stimuli reduced the goodness-of-fit measures, but fits to prediction were still reasonably good. The virtual factor weighting was 0.2 ± 0.02 *SEM* for the arrow-junction illusion and 0.5 ± 0.03 *SEM* for the fork-junction illusion.

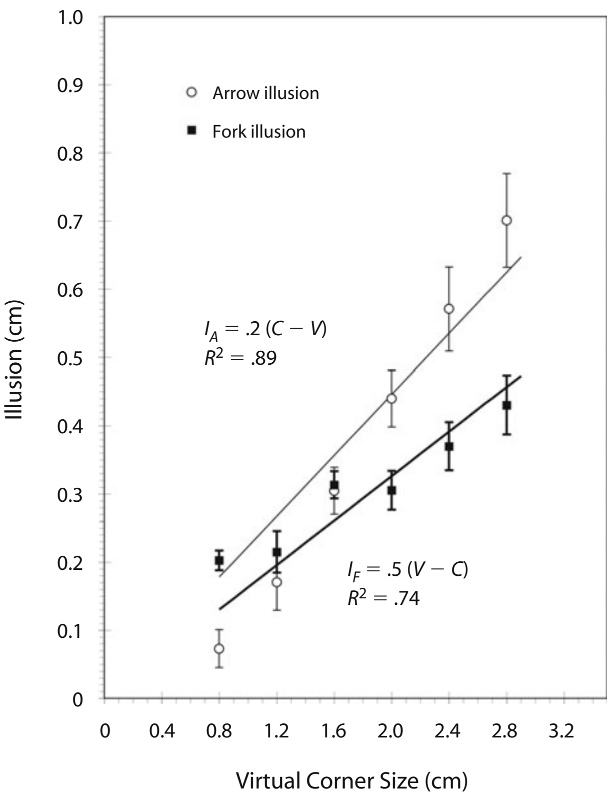

Figure 4. Experiment 1: Arrow- and fork-junction illusions as a function of virtual corner size for projections of convex and concave corners, respectively. Equation parameters and goodness-of-fit measures are shown for each data illusion.

The influence of the virtual factor was greater for the fork-junction illusion than for the arrow-junction illusion. On average, the arrow-junction illusion, 0.4 cm ± 0.02 *SEM*, was about 10% of the control value, and the fork-junction illusion, 0.3 cm ± 0.01 *SEM*, was about 26% of the control value; but the fork-junction illusion was about 18% smaller than the arrow-junction illusion.

Discussion

These results demonstrate the viability of the present methodology and suggest that the only factor producing the illusions was virtual corner size. Moreover, although the arrow-junction illusion was larger for the present stimuli, the larger weighting of the virtual factor is consistent with the usual finding of an illusion larger than that for the arrow-junction stimuli. For the present stimuli (see Figure 3), on average, the arrow-junction stimuli were 1.8 cm larger than virtual corner size, and the fork-junction stimuli were 0.6 cm smaller than the virtual corner size. The larger weighting of virtual size was not sufficient to produce a fork-junction illusion greater than that produced by the smaller weighting of virtual size for arrow-junction stimuli. As will be seen in the following experiments, the larger weighting for concave corners produces a larger fork-junction illusion when the difference between drawn and virtual size is more comparable for arrow-junction and fork-junction stimuli.

EXPERIMENT 2
Virtual Station Point

The first experiment was unusual in that the projected corner edge or interior target line was not the same size for each pair of experimental stimuli. Experiment 2 adopted the more common practice of equating projective size for each pair of experimental stimuli and manipulated another virtual factor. Station point distance from the picture plane (the point from which the virtual corners were drawn) was manipulated, whereas the projected size of the corner edge or interior target line was held constant by varying virtual corner size. In general, it may be expected that station point recovery and illusion magnitude should be greater, the smaller the difference from the vantage point from which the stimuli are viewed; for example, maximal illusion would occur if the vantage point was the same as the station point.

Method

Virtual corner station point was manipulated, and projected size of the corner edge was held constant at 3.2 cm. Levels of station point distance were 1.0, 2.0, 3.0, and 4.0 cm, requiring virtual corner sizes of 0.6, 1.9, 2.4, and 2.6 cm, respectively, for convex corner drawings and 5.8, 4.5, 4.1, and 3.8 cm for concave corner drawings, respectively. These stimuli are illustrated in Figure 5. Groups of 42 subjects were assigned to each level of station point distance, for a total of 168.

Other drawing characteristics were, in order of increasing station point distance for convex and concave corner drawings, respectively: interior angles of 32º, 51º, 62º, 68º, and 148º, 129º, 118º, 112º; projected boundary line lengths of 1.5, 1.0, 0.9, and 0.9 cm for both corners; projected distances between boundary line terminations were the same as corner size; projected maximal width was constant at 1.6 cm.

The nine practice stimuli were 0.8 to 5.6 cm in 0.6-cm increments, and the four filler stimuli were 1.0, 2.1, 4.3, and 5.4 cm. The single control stimulus was 3.2 cm, stopped by T junctions (see the General Method section). The two experimental stimuli were presented twice in each block of trials, and data were averaged.

Results

Normalization of the data to control values produced, on average, an addition of 0.01 cm ± 0.03 *SEM*, indicating a small tendency toward underestimation. Normalized reproduced size data were well fit for convex corners ($R^2 = .86$) and concave corners ($R^2 = .93$) by Equation 1 (see the General Method section) with the sum of virtual and drawing weights constrained to equal 1. Because virtual factor weightings were similar, the contribution of both virtual and drawn size to the illusions was assessed using constrained Equations 2 and 3, as illustrated in Figure 6. As can be seen, fit to prediction was good and taking the difference between reproduced size and a control constant did not reduce the goodness of fit. The virtual factor and drawing weightings, respectively, were 0.2 ± 0.04 *SEM* and 0.8 ± 0.03 *SEM* for the arrow-junction illusion, and 0.3 ± 0.04 *SEM* and 0.7 ± 0.06 *SEM* for the fork-junction illusion.

The influence of the virtual factor was again greater for the fork-junction illusion than for the arrow-junction illusion. On average, the arrow-junction illusion, 0.3 cm ± 0.02 *SEM*, was about 8% of the control value; the fork-junction illusion, 0.4 cm ± 0.03 *SEM*, was about 12% of the control value; and the fork-junction illusion was about 43% larger than the arrow-junction illusion.

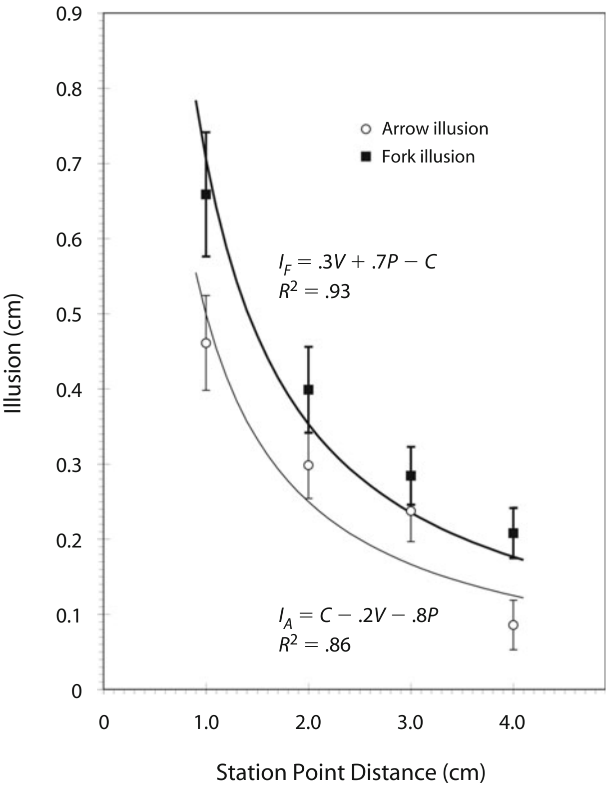

Figure 6. Experiment 2: Arrow- and fork-junction illusions as a function of station point distance for projections of convex and concave corners, respectively. Equation parameters and goodness-of-fit measures are shown for each data illusion.

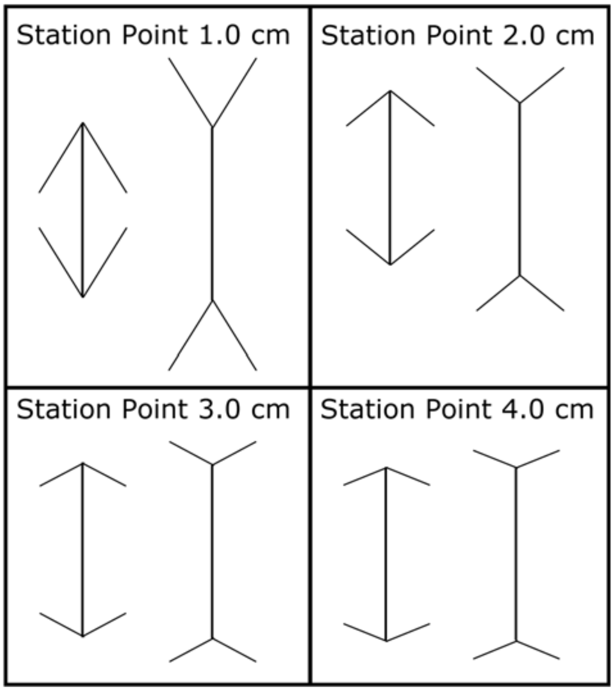

Figure 5. Experiment 2 stimuli as a function of station point distance.

Discussion

Even though the drawn size of each pair of experimental stimuli was the same, the illusions followed the varying virtual corner size. Experiment 2 replicated the first experiment in producing a larger virtual factor weighting for the larger fork-junction illusion. Moreover, the fork-junction illusion was the larger illusion, as is usually the case, and as expected when the difference between drawn and virtual size is comparable, on average, for arrow-junction (1.3 cm) and fork-junction stimuli (1.4 cm). These data further demonstrate the viability of the present methodology for more traditional experimental stimuli.

EXPERIMENT 3
Virtual Station Point

In this experiment, the generality of the results for Experiment 2 was tested. Experiment 3 manipulated the station point distance from the picture plane, the point from which the virtual corners were drawn; in contrast with Experiment 2, it held the virtual corner size constant, causing the projected size of the corner edge or interior target line to vary.

Method

Virtual corner station point was manipulated and corner size was held constant at 1.6 cm for convex corners, and 4.8 cm for concave corners. Levels of station point distance were 1.2, 2.2, 3.2, and 4.2 cm, with projecting interior target line sizes of 4.8, 2.5, 2.1, and 2.0 cm, respectively, for convex corner drawings and 2.9, 3.5, 3.8, and 4.0 cm for concave corner drawings. These stimuli are illustrated in Figure 7. Groups of 51, 54, 48, and 51 subjects were assigned to increasing levels of station point distance, respectively, for a total of 204 subjects.

Other drawing characteristics were, in order of increasing station point distance for convex and concave corner drawings, respectively: interior angles of 27º, 60º, 72º, 77º, and 140º, 129º, 121º, 116º; projected boundary line lengths of 1.8, 0.9, 0.8, 0.8 and 1.2, 1.0, 0.9, 0.9 cm; projected distances between boundary line terminations were the same as corner size; projected maximal width was constant at 1.6 cm for convex corner drawings and 4.8 cm for concave corner drawings.

The nine practice stimuli were 0.8 to 5.6 cm in 0.6-cm increments, and the five filler stimuli were 1.0, 2.1, 3.2, 4.3, and 5.4 cm. The two control stimuli were the size of projected target lines in the two experimental stimuli, but stopped by T junctions (see the General Method section).

Results

Normalization of the data to control values produced, on average, an addition of 0.07 cm ± 0.03 *SEM*, indicating a small tendency toward underestimation. Normalized reproduced size data were well fit for both corners ($R^2 = .99$) by Equation 1 (see the General Method section) with the sum virtual and drawing weights constrained to equal 1. As in the previous experiment, Equations 2 and 3 were used to show the contribution of both virtual and drawn size to the illusions, as illustrated in Figure 8. As can be seen, fit to prediction was good, and taking the difference between reproduced size and the various controls only slightly reduced the goodness of fit. The virtual and drawing factor weightings, respectively, were 0.2 ± 0.09 *SEM* and 0.8 ± 0.05 *SEM* for the arrow-junction illusion, and 0.3 ± 0.04 *SEM* and 0.7 ± 0.05 *SEM* for the fork-junction illusion.

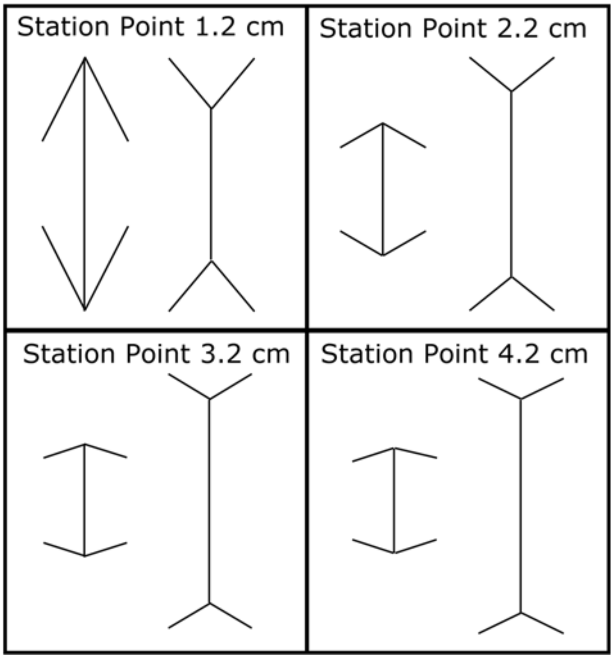

Figure 7. Experiment 3 stimuli as a function of station point distance.

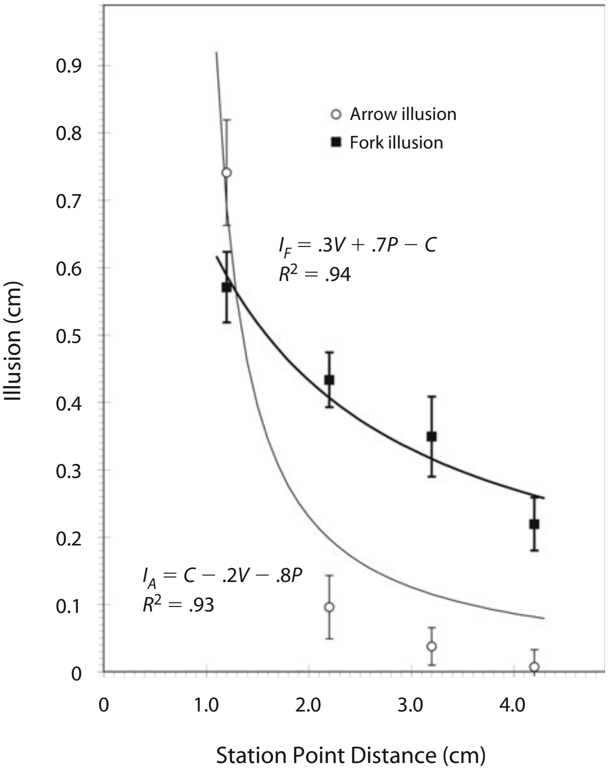

Figure 8. Experiment 3: Arrow- and fork-junction illusions as a function of station point distance for projections of convex and concave corners, respectively. Equation parameters and goodness-of-fit measures are shown for each data illusion.

The influence of the virtual factor was yet again greater for the fork-junction illusion than for the arrow-junction illusion. On average, the arrow-junction illusion, 0.2 cm ± 0.03 *SEM*, was about 8% of the control value; the fork-junction illusion, 0.4 cm ± 0.02 *SEM*, was about 11% of the control value; and the fork-junction illusion was about 78% larger than the arrow-junction illusion.

Discussion

These results show how the constant virtual corner size modulates the varying projective size of the corner edge or interior target line, similar to the reversed relationship in Experiment 2. Again, the results replicate the previous experiments in producing the same virtual factor weightings for arrow- and fork-junction illusions (Experiment 2), with the larger weighting going to the larger fork-junction illusion (Experiments 1 and 2). Note than the larger weighting was sufficient to produce a larger fork-junction illusion even though, on average, the difference between drawn and virtual size was greater for arrow-junction stimuli (2.4 cm) than for fork-junction stimuli (1.3 cm).

EXPERIMENT 4
Virtual Corner Depth

Experiment 4 manipulated another feature of virtual corners, corner depth or the distance from the corner edge to the picture plane, whereas the boundary line terminations remained in the picture plane. Corner height was held constant, whereas projected size of the projected edge (target line) varied with corner depth. The primary purpose of this experiment was to further test the generality of Hypothesis 1 when the drawn distance between boundary line terminations was held constant, rather than covarying with corner size, as in all previous experiments.

Method

Virtual corner depth from the picture plane was manipulated, while holding constant corner height at 1.6 cm for convex corners and 4.8 cm for concave corners. Levels of corner distance were 0.3, 0.5, 0.7, 0.9, and 1.1 cm, producing projected sizes of the corner edge or interior target line of 2.0, 2.3, 2.8, 3.7, and 5.1 cm, respectively, for convex corner drawings, and 4.0, 3.7, 3.3, 3.1, and 2.8 cm, respectively, for concave corner drawings. These stimuli are illustrated in Figure 9. Groups of 26, 20, 26, 21, and 25 subjects were assigned to increasing levels of corner distance, respectively, for a total of 118 subjects.

Other drawing characteristics were, in order of increasing corner distance for convex and concave corner drawings, respectively: interior angles of 58º, 54º, 48º, 41º, and 32º, and 142º, 139º, 136º, 134º, and 132º, and projected boundary line lengths of 0.4, 0.6, 0.9, 1.4, and 2.1 cm, and 0.5, 0.8, 1.0, 1.2, and 1.5 cm. Projected distance between boundary line terminations was 1.6 and 4.8 cm for convex and concave corners, respectively, and projected width was 0.6, 1.0, 1.4, 1.8, and 2.2 cm with increasing distance from the picture plane for both corner types.

The nine practice stimuli, respectively, for increasing corner distance, were: 0.8, 1.4, 2.0, 2.5, 3.0, 3.5, 4.0, 4.6, and 5.2 cm; 1.1, 1.7, 2.3, 2.7, 3.0, 3.3, 3.7, 4.3, and 4.9 cm; 1.6, 2.2, 2.8, 3.0, 3.1, 3.2, 3.3, 3.9, and 4.9 cm; 1.9, 2.5, 3.1, 3.2, 3.4, 3.5, 3.7, 4.3, and 4.9 cm; and 1.6, 2.2, 2.8, 3.4, 4.0, 4.6, 5.1, 5.7, and 6.3 cm. The five filler stimuli were the same as the middle five practice stimuli for the corresponding corner distance. The two control stimuli were the size of the target lines in the two experimental stimuli, stopped by T junctions (see the General Method section).

Results

Normalization of the reproduced size data to control values produced, on average, an addition of 0.03 cm ± 0.03 *SEM*, indicating a small tendency toward underestimation. The normalized data were well fit by constrained Equation 1 (see the General Method section), yielding $R^2 = .99$ and $R^2 = .95$ for the convex and concave corner, respectively. Constrained Equations 2 and 3 were used to assess the contributions of virtual and context-drawing factors to the illusions, as illustrated in Figure 10. As can be seen, finding the difference between reproduced size data and a constant did not substantially affect the goodness-of-fit measures for either the arrow-junction illusion, $R^2 = .93$, or the fork-junction illusion, $R^2 = .95$. The virtual and target-drawing weighting factors were, respectively, 0.2 ± 0.06 *SEM* and 0.8 ± 0.03 *SEM* for the arrow-junction illusion, and 0.3 ± 0.03 *SEM* and 0.7 ± 0.04 *SEM* for the fork-junction illusion.

As in preceding experiments, the influence of the virtual factor was greater for the fork-junction illusion than for the arrow-junction illusion. On average, the arrow-junction illusion, 0.3 cm ± 0.04 *SEM*, was about 10% of the control value; the fork-junction illusion, 0.4 cm ± 0.03 *SEM*, was about 13% of the control value; and the fork-junction illusion was about 59% larger than the arrow-junction illusion.

Discussion

As in the previous experiments, results were consistent with Hypothesis 1. Again, the results replicate the previous experiments in producing the same virtual factor weightings for arrow- and fork-junction illusions (Experiments 2 and 3), with the larger weighting going to the larger fork-junction illusion (Experiments 1, 2, and 3).

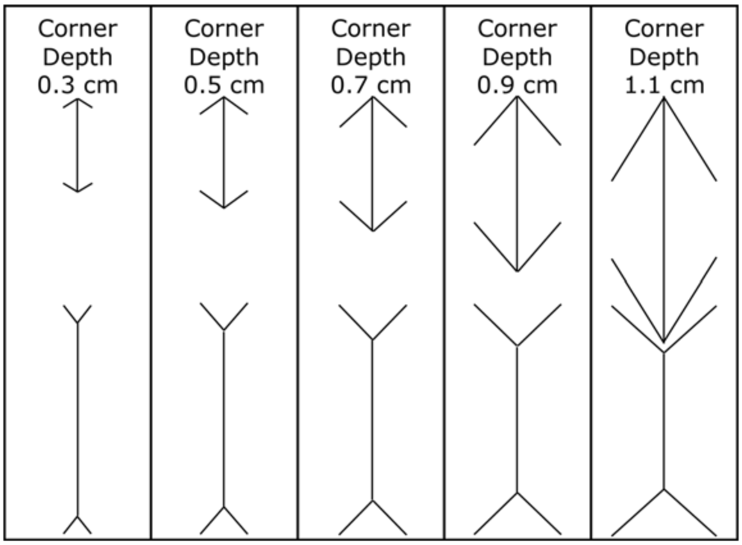

Figure 9. Experiment 4 stimuli as a function of virtual corner depth.

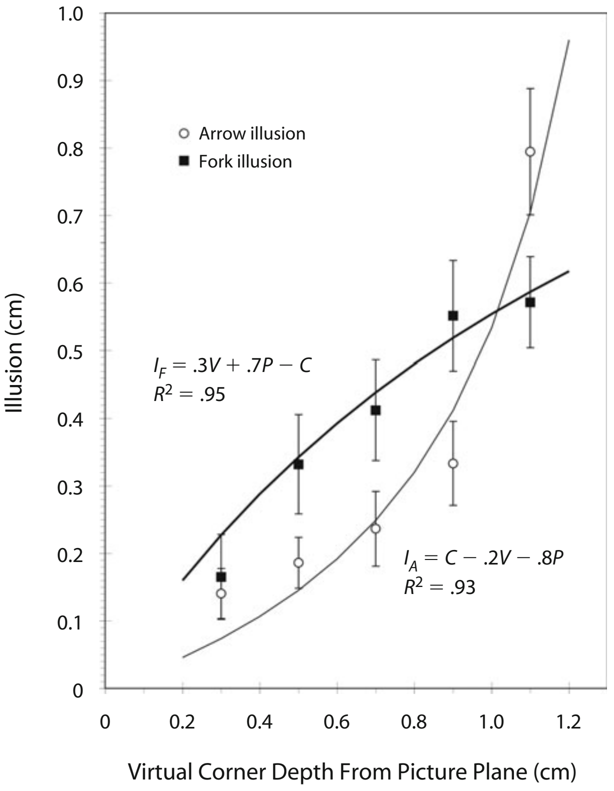

Figure 10. Experiment 4: Arrow- and fork-junction illusions as a function of corner depth from the picture plane for projections of convex and concave corners, respectively. Equation parameters and goodness-of-fit measures are shown for each data illusion.

EXPERIMENT 5
Virtual Corner Distance

In the first three experiments, virtual corner size was confounded with the drawing factor of projected distance between boundary line terminations because the boundary lines always terminated in the picture plane and therefore marked off in the drawing the virtual corner size. Results from Experiment 4, where this drawing factor was held constant, suggest that it may be important, especially for the fork-junction illusion. When we moved the virtual corners away from the picture plane, the projected distance between boundary line terminations varied at a different rate from virtual corner size, and the contribution of this second drawing factor could be separately assessed. Three hypotheses were evaluated: (1) Virtual corner size is the sole determinant of the illusions (Hypothesis 1, Equation 1), (2) context drawing size is the sole determinant of the illusions (Hypothesis 2, Equation 6), and (3) both factors contribute to the illusions (Hypothesis 3, Equation 7).

Method

Virtual corner distance from the station point was manipulated, corner depth was held constant at 0.8 cm, and corner size was held constant at 1.6 cm for convex corners and 4.8 cm for concave corners. Levels of corner distance were 0.3, 0.5, 0.7, 0.9, and 1.1 cm, producing projected sizes of the corner edge or interior target line of 2.0, 2.3, 2.8, 3.7, and 5.1 cm, respectively, for convex corner drawings and 4.9, 3.7, 3.3, 3.1, and 2.8 cm for concave corner drawings, respectively. These stimuli are illustrated in Figure 11. Groups of 26, 25, 25, 24, and 25 subjects were assigned to increasing levels of corner distance, for a total of 125 subjects.

Other drawing characteristics were, in order of increasing corner distance for convex and concave corner drawings, respectively: interior angles of 58º, 54º, 48º, 41º, 32º, and 142º, 139º, 136º, 134º, 132º; projected boundary line lengths of 0.7, 0.8, 1.0, 1.3, and 2.0 cm and 1.9, 1.5, 1.2, 1.0, and 0.9 cm; projected distances between boundary line terminations of 1.2, 1.3, 1.5, 1.7, and 2.0 cm and 7.0, 5.9, 5.1, 4.5, and 4.0 cm; and projected widths of 1.2, 1.3, 1.5, 1.7, and 2.0 cm and 2.3, 2.0, 1.7, 1.5, and 1.3 cm.

The nine practice stimuli, for increasing corner distance, respectively, were: 0.8, 1.4, 2.0, 2.5, 3.0, 3.5, 4.0, 4.6, and 5.2 cm; 1.1, 1.7, 2.3, 2.7, 3.0, 3.3, 3.7, 4.3, and 4.9 cm; 1.6, 2.2, 2.8, 3.0, 3.1, 3.2, 3.3, 3.9, and 4.9 cm; 1.9, 2.5, 3.1, 3.2, 3.4, 3.5, 3.7, 4.3, and 4.9 cm; and 1.6, 2.2, 2.8, 3.4, 4.0, 4.6, 5.1, 5.7, and 6.3 cm. The five filler stimuli were the same as the middle five practice stimuli for the corresponding corner distance. The two control stimuli were the size of the target lines in the two experimental stimuli, stopped by T junctions (see the General Method section).

Results

Normalization of the data to control values produced, on average, an addition of 0.07 cm ± 0.03 *SEM*, indicating a small tendency toward underestimation. The normalized reproduced size data for convex and concave corners were best fit, with smallest parameter variability, by different equations.

Reproduced size data for the convex corner were best fit with the smallest parameter variability by the Virtual Structure Hypothesis 1, $R^2 = .99$, with virtual and target-drawing factor weightings, respectively, of 0.2 ± 0.08 *SEM* and 0.8 ± 0.04 *SEM*. Fit for the Drawing Structure Hypothesis 2 was $R^2 = .98$, with context- and target-drawing factor weightings, respectively, of 0.2 ± 0.23 *SEM* and 0.8 ± 0.11 *SEM*. Fit for the combined Virtual and Drawing Structure Hypothesis 3 was $R^2 = .99$, with virtual, context-drawing, and target-drawing factor weightings, respectively, of 0.3 ± 0.75 *SEM*, −0.1 ± 1.48 *SEM*, and 0.8 ± 0.35 *SEM*.

Reproduced size data for the concave corner were best fit by the combined Virtual and Drawing Structure Hypothesis 3, $R^2 = .99$, with virtual, context-drawing, and target-drawing factor weightings, respectively, of 0.2 ± 0.15 *SEM*, 0.1 ± 0.23 *SEM*, and 0.7 ± 0.58 *SEM*. Fit for the Drawing Structure Hypothesis 2 was $R^2 = .92$, with context- and target-drawing factor weightings, respectively, of 0.2 ± 0.19 *SEM* and 0.8 ± 0.31 *SEM*. Fit for the Virtual Structure Hypothesis 1 was $R^2 = .86$, with virtual and target-drawing factor weightings, respectively, of 0.3 ± 0.16 *SEM* and 0.7 ± 0.22 *SEM*. Parameter variability was less for the single-factor hypotheses, whereas goodness of fit was only slightly better for the two-factor hypothesis; however, the single-factor hypotheses were rejected, consistent with results for the fork-junction illusion (see below).

As can be seen in Figure 12, taking the difference between reproduced sizes and varying controls reduced the goodness-of-fit measures, but the illusions were best fit with smallest parameter variability by the same equations as were the reproduced size data.

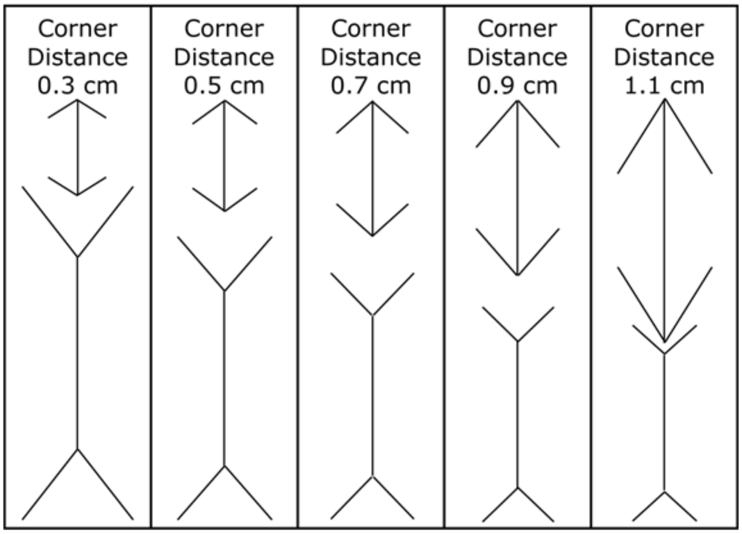

Figure 11. Experiment 5 and 6 stimuli as a function of corner picture plane distance.

The arrow-junction illusion data were best fit with smallest parameter variability by the Virtual Structure Hypothesis 1, $R^2 = .95$, with virtual and target-drawing factor weightings, respectively, of 0.2 ± 0.06 *SEM* and 0.8 ± 0.03 *SEM*. Fit for the Drawing Structure Hypothesis 2 was $R^2 = .88$, with context- and target-drawing factor weightings, respectively, of 0.2 ± 0.19 *SEM* and 0.08 ± 0.09 *SEM*. Fit for the combined Virtual and Drawing Structure Hypothesis 3 was $R^2 = .96$, with virtual, context-drawing, and target-drawing factor weightings, respectively, of 0.3 ± 0.52 *SEM*, −0.1 ± 1.03 *SEM*, and 0.8 ± 0.24 *SEM*.

The fork-junction illusion data were only fit by the combined Virtual and Drawing Structure Hypothesis 3: $R^2 = .27$, with virtual, context-drawing, and target-drawing factor weightings, respectively, of 0.2 ± 0.46 *SEM*, 0.1 ± 0.73 *SEM*, and 0.7 ± 1.79 *SEM*. Fit for both the Drawing Structure Hypothesis 2 and the Virtual Structure Hypothesis 1 produced negative R^2s, indicating inappropriate models.

In the present data, the virtual factor appears to be the sole determinant of the arrow-junction illusion, but both virtual and context-drawing factors contributed to the fork-junction illusion. On average, the arrow-junction illusion, 0.3 cm ± 0.04 *SEM*, was about 9% of the control value; the fork-junction illusion, 0.5 cm ± 0.03 *SEM*, was about 15% of the control value; and the fork-junction illusion was about 263% larger than the arrow-junction illusion, reflecting the additional factor.

Discussion

Reproduced size data for the convex corner arrow-illusion data were maximally fit with only the virtual factor and the drawing factor of projected corner edge (interior target line). Inclusion of the second drawing factor of projected distance between boundary line terminations was necessary to produce the best fit for the reproduced size data for the concave corner, and an appropriate model for the fork-junction illusion. The small size of the fit measure and high variability of parameter estimates for the fork-junction illusion is to be expected from the addition of opposing virtual and context-drawing factors. These data suggest an explanation for the traditionally larger fork-junction illusion. Both illusions reflect the same contributions from the virtual factor, but the fork-junction illusion reflects additional contribution of the context-drawing factor.

EXPERIMENT 6
Virtual Corner Distance

Experiment 6 tested the generality of Experiment 5 results for different viewing times. The method was the same as in Experiment 5, except that subjects viewed the stimulus array for 150, 250, 500, or 1,000 msec, different-sized groups of 43, 100, 97, and 51 subjects for the four viewing times, respectively, for a total of 291 subjects. Within viewing times, the number of subjects receiving the five distances of the virtual corner from the picture plane, respectively, was 9, 9, 9, 8, and 8 for the first viewing time; 20, 20, 20, 20, and 20 for the second viewing time; 19, 20, 18, 20, and 20 for the third viewing time; and 10, 9, 12, 9, and 11 for the fourth viewing time.

Results

Normalization of the data to control values produced, on average, an addition of 0.14 cm ± 0.02 *SEM*, indicating on average a slight tendency toward underestimation. An ANOVA revealed the same pattern of statistical reliability for both the normalized reproduced size and illusion data. For example, the only reliable effects were main effects of illusion [$F(1,271) = 50.26$, $p < .001$] and virtual corner distance [$F(4,271) = 19.90$, $p < .001$], and the interaction of illusion and virtual corner distance [$F(4,271) = 11.85$,

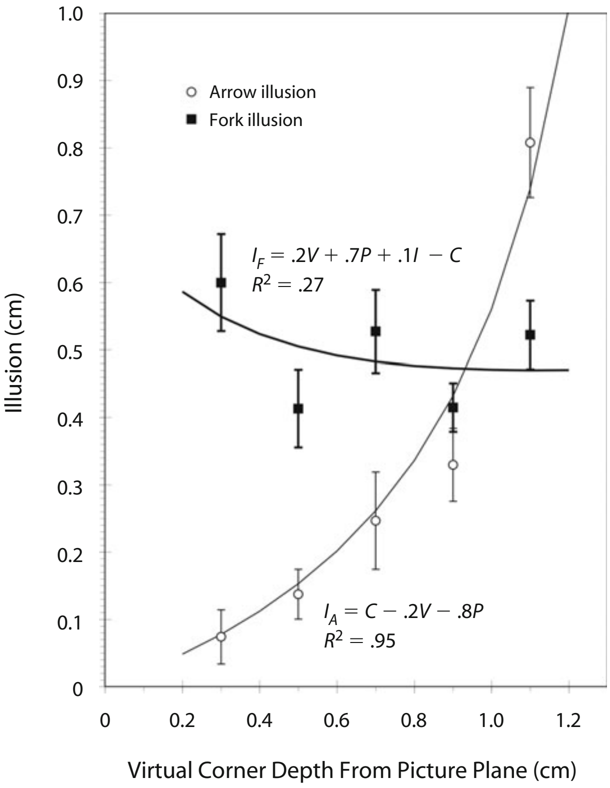

Figure 12. Experiment 5: Arrow- and fork-junction illusions as a function of corner distance from picture plane for projections of convex and concave corners, respectively. Equation parameters and goodness-of-fit measures are shown for each data illusion.

$p < .001$]. Viewing time was not a significant source of variance ($p > .361$) and, therefore, was not further analyzed. The only effect of manipulating viewing time appears to have been to increase random variability.

Normalized reproduced size data for the convex corner were best fit with the smallest parameter variability by the Virtual Structure Hypothesis 1, $R^2 = .99$, with virtual and target-drawing factor weightings, respectively, of 0.2 ± 0.05 *SEM* and 0.8 ± 0.02 *SEM*. Fit for the Drawing Structure Hypothesis 2 was $R^2 = .99$, with context- and target-drawing factor weightings, respectively, of 0.2 ± 0.18 *SEM* and 0.8 ± 0.09 *SEM*. Fit for the combined Virtual and Drawing Structure Hypothesis 3 was $R^2 = .99$, with virtual, context-drawing, and target-drawing factor weightings, respectively, of 0.3 ± 0.36 *SEM*, −0.1 ± 0.70 *SEM*, and 0.8 ± 0.17 *SEM*. Goodness of fit was only nominally different for the three hypotheses, but parameter variability was lowest for the Virtual Structure Hypothesis.

Normalized reproduced size data for the concave corner were best fit by the combined Virtual and Drawing Structure Hypothesis 3, $R^2 = .95$, with virtual, context-drawing, and target-drawing factor weightings, respectively, of 0.2 ± 0.70 *SEM*, 0.1 ± 1.10 *SEM*, and 0.7 ± 2.69 *SEM*. Fit for the Drawing Structure Hypothesis 2 was $R^2 = .76$, with context- and target-drawing factor weightings, respectively, of 0.3 ± 0.32 *SEM* and 0.7 ± 0.50 *SEM*. Fit for the Virtual Structure Hypothesis 1 was $R^2 = .81$, with virtual and target-drawing factor weightings, respectively, of 0.4 ± 0.18 *SEM* and 0.6 ± 0.25 *SEM*. Parameter variability was less for the single-factor hypotheses, whereas goodness of fit was better for the two-factor hypothesis; moreover, rejection of the single-factor hypotheses is consistent with the results for the fork-junction illusion (see below).

As can be seen in Figure 13, taking the difference between reproduced sizes and varying controls reduced the goodness-of-fit measures, but the illusions were best fit by the same hypotheses as the reproduced size data.

The arrow-junction illusion data were best fit with smallest parameter variability by the Virtual Structure Hypothesis 1, $R^2 = .96$, with virtual and target-drawing factor weightings, respectively, of 0.2 ± 0.06 *SEM* and 0.8 ± 0.03 *SEM*. Fit for the Drawing Structure Hypothesis 2 was $R^2 = .88$, with context- and target-drawing factor weightings, respectively, of 0.2 ± 0.19 *SEM* and 0.8 ± 0.10 *SEM*. Fit for the combined Virtual and Drawing Structure Hypothesis 3 was $R^2 = .97$, with virtual, context-drawing, and target-drawing factor weightings, respectively, of 0.3 ± 0.45 *SEM*, −0.1 ± 0.88 *SEM*, and 0.8 ± 0.21 *SEM*. Goodness of fit was nominally better for the two-factor hypothesis, but parameter variability was much larger.

The fork-junction illusion data were only fit by the combined Virtual and Drawing Structure Hypothesis 3: $R^2 =$

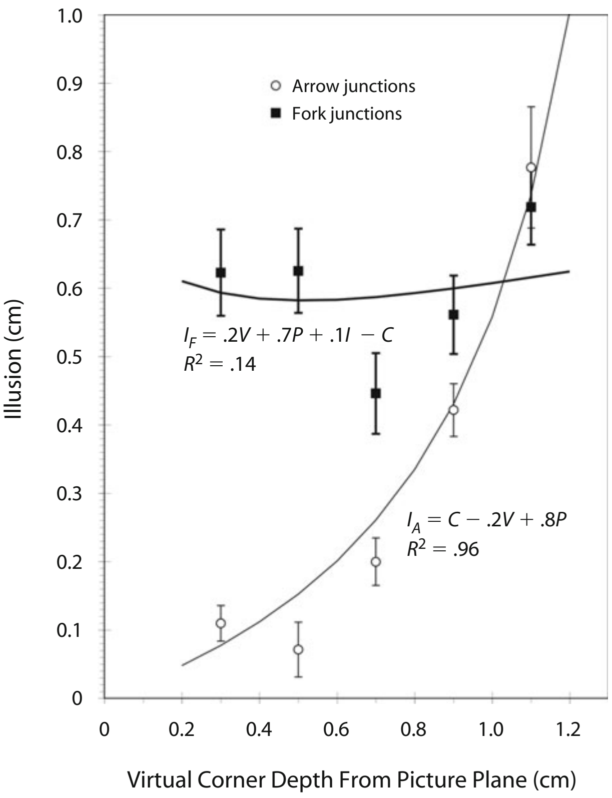

Figure 13. Experiment 6: Arrow- and fork-junction illusions as a function of corner distance from picture plane for projections of convex and concave corners, respectively. Equation parameters and goodness-of-fit measures are shown for each data illusion.

.14, with virtual, context-drawing, and target-drawing factor weightings, respectively, of 0.2 ± 0.62 *SEM*, 0.1 ± 0.98 *SEM*, and 0.7 ± 2.42 *SEM*. Fit for both the Drawing Structure Hypothesis 2 and the Virtual Structure Hypothesis 1 produced negative R^2s, indicating inappropriate models.

In the present data, the virtual factor appears to be the sole determinant of the arrow-junction illusion, but both virtual and context-drawing factors contributed to the fork-junction illusion. On average, the arrow-junction illusion, 0.3 cm ± 0.03 *SEM*, was about 10% of the control value; the fork-junction illusion, 0.6 cm ± 0.03 *SEM*, was about 18% of the control value; and the fork-junction illusion was about 88% larger than the arrow-junction illusion, reflecting the additional factor.

Discussion

Reproduced size data for the convex corner arrow-illusion data were fit with only the virtual factor and the drawing factor of projected corner edge (interior target line). Inclusion of the second drawing factor of projected distance between boundary line terminations was necessary to produce a fit for the reproduced size data for the concave corner and an appropriate model for the fork-junction illusion. The small size of the fit measure and the high variability of parameter estimates for the fork-junction illusion are to be expected from the addition of opposing virtual and context-drawing factors. These data replicate those of Experiment 5, showing generality over viewing time, and support the conclusion that both illusions reflect the same contributions from the virtual factor, but the fork-junction illusion reflects the additional contribution of the context-drawing factor.

GENERAL DISCUSSION

These results suggest that the virtual source of bias assumed to be the basis of the illusions by scene-based (linear perspective bias) and picture-based (picture plane bias) theories can be identified. Moreover, virtual and drawn factors appear to combine in a simple additive fashion. For the first four experiments, reproduced size was well predicted by the weighted sum of the virtual and picture plane structure, and the illusions were well predicted by the weighting found for the biasing source. Moreover, the relative weighting conformed to the general finding that the fork-junction illusion is larger in magnitude than the arrow-junction illusion (Binet, 1895; Christie, 1975; Day & Dickinson, 1976; Erlebacher & Sekuler, 1974; Heymans, 1896; Piaget, 1961/1969). The finding that, on average, the fork-junction stimulus was perceived to be about 80% larger than the arrow-junction stimulus is well beyond the upper end of the usual range of 25% to 30% (Coren & Girgus, 1978a, 1978b), which may reflect the use of stimuli that were projections of the underlying virtual structures for the two illusions.

Results from the last two experiments illustrate the ability of the present methodology to analyze multiple contributions to the illusions. When virtual structure and the second drawing factor—projected distance between boundary line terminations predicted by object-based theories—were manipulated separately, the factor contributions were found to be different for the two illusions. The arrow-junction illusion appears to be solely the result of virtual structure bias, but the fork-junction illusion seems to further involve the drawing context in which the target line appears. These contrasting results suggest that the traditionally larger fork-junction illusion arises from additional contribution from the drawing context. Moreover, presence of both virtual and drawing structure components in Experiments 5 and 6 supports the conclusion that virtual structure effects identified in the first four experiments cannot be attributed to confounded drawing structure.

The nature of the virtual bias portion of the illusions remains unclear. The present data do not permit a clear decision between picture-based theory and scene-based theory. However, picture-based theory seems to face greater difficulties than does scene-based theory.

Picture-based theory faces the formidable problem of solving the inverse perspective problem. Previous work (e.g., Barrow & Tenenbaum, 1981; Biederman, 1995; Binford, 1981; Clowes, 1971; Malik, 1987; Sugihara, 1984; Waltz, 1975) detailing the constraints that permit recovery of 3-D shape from line drawings might be extended to include recovery of size and depth metric. However, such development for the minimal perspective Müller-Lyer drawings is challenging, all the more so because available data suggest that constraints must be identified for isolated three-line junctions (Day & Dickinson, 1976; Predebon, 1994, 2000; Redding & Hawley, 1993; Warren & Bashford, 1977), not just for the complete Müller-Lyer drawings.

A related problem for picture-based theory is that the size distortion is graded; it is greatest in the vicinity of the line junctions, and decreases with increasing distance therefrom (Heymans, 1896; Morgan et al., 1990; Restle & Decker, 1977; Warren & Bashford, 1977), confirming the requirement that recovery of virtual structure be accomplished for isolated junctions. It has been suggested that the graded nature of the illusion is also a problem for scene-based theory, which seems to require holistic size scaling (Morgan et al., 1990). However, Gregory (1965, 1967) has argued that very local perspective features can set primary constancy scaling (see also Redding & Hawley, 1993).

Perhaps the greatest difficulty facing scene-based theory is the larger magnitude of the fork-junction illusion. Gillam (1978) attributes this usual finding to differential placement of the orthogonalization pivot point, as illustrated in Figure 14. Assuming the trapezoidal figure to be the natural perspective projection of an in-depth rectangle, orthogonalization operates to change the figure toward a rectangle, changing acute and obtuse angles toward right angles. Gillam (1978) notes that orthogonalization around points P_2 would produce equal shortening of line P_1P_1 and lengthening of line P_3P_3: that is, equal arrow-junction and fork-junction illusions. Changing the pivot point toward P_1 decreases the arrow-junction illusion and increases the fork-junction illusion, whereas changing the pivot point toward P_3 increases the arrow-

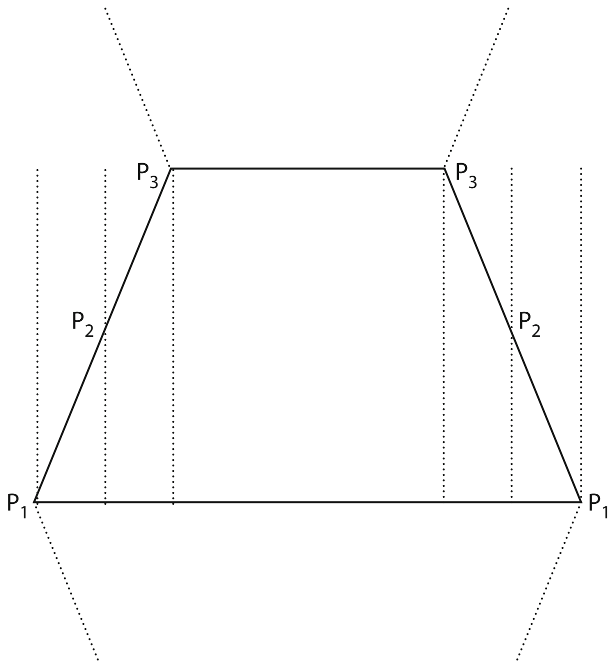

Figure 14. Illustration of Gillam's (1978) orthogonalization account of illusion asymmetry. The trapezoidal figure represents the natural perspective projection of a rectangle, and orthogonalization tends to increase acute angles and decrease obtuse angles. Rotation around points between P_1 and P_2 would produce fork-junction illusions greater than arrow-junction illusions. See text for additional explanation. (After Gillam, 1978, Figure 6.4, p. 62.)

junction illusion and decreases the fork-junction illusion. Therefore, a pivot point somewhere between P_2 and P_1 would produce the typically larger fork-junction illusion. However, Gillam offers no argument for why this should consistently be the case. The present hypothesis is that the usually larger fork-junction illusion can be attributed to the additional contribution from the drawing context, "interwingtip distance," of object-based theory. The results of Experiments 5 and 6 support the conclusion of a drawing context component for the fork-junction illusion, but not the arrow-junction illusion.

The most extensively developed object-based theory is Pressey's assimilation hypothesis (Pressey, 1970, 1972, 1974; Pressey & Pressey, 1992; cf. Sekuler & Erlebacher, 1971). The present data suggest that attribute averaging may contribute especially to the fork-junction illusion, but the conditions for such contribution remain unclear. Moreover, Pressey's hypothesis suffers from a lack of clear connections with the larger body research on object perception (e.g., Biederman, 1987, 1995; Biederman & Cooper, 1992; Biederman & Gerhardstein, 1993; Yue, Vessel, & Biederman, 2007) and, consequently, gives the appearance of ad hoc assumptions. Attribute averaging is a clear example of how object representation can bias judgment of selected attributes and articulation of such connections can enhance the quality of object-based theories. Such theories seem particularly appropriate for illusions where the stimulus arrays have no natural or linear perspective (Coren & Girgus, 1978a; Day, 1972).

Finally, it should be recognized that the present approach and data are consistent with the view that the Müller-Lyer illusions likely arise from many sources (see Coren & Girgus, 1978a, 1978b). The illusions in their many forms of the Müller-Lyer stimuli (e.g., Day, 1972; DeLucia & Hochberg, 1991) likely include several processes, including, but not limited to, those articulated here. The present method of constraining stimulus arrays by possible virtual structures can facilitate identification of contributing stimulus attributes arising from virtual structure, thereby enabling discovery of other contributing processes.

AUTHOR NOTE

We thank Rebecca Dieken, Jennifer Ginsberg, Tonja Jameson, Mindy Maher, Erin Mars, Angela Roberto, and Brittany Stevenson for their assistance in data collection for the present experiments. The authors also thank the following people for their help over the several years during which the present ideas were developed: Lisa Alumbaugh, Emily Ashpole, Mary Bivona, Jennifer Bonomo, Denny Brackett, Chris Casey, Crystal Champion, Kathleen Craven, Brett Davenport, Frank D'Antuono, Sheryl Demott, Julie Douglas, Amber Elledge, Gina Gerloff, Jennifer Hankins, Danielle Harper, Erik Hawley, Jean Huck, Brenda Iverson, Ronald Jacobs, Heather Johnson, Paula Kern, Alissa Kramen, Cheri Kubitz, Karen Lonquist, Carrigan Manetti, Paul Martin, Meghan Moore, Sonja Parkinson, Bret Phillips, Natalie Plenys, Zed Rogers, Deborah Scherr, Amy Sheldon, Kim Starkweather, Carly Stein, Gregory Stromski, Richard Temple, Brian Unterreiner, and Georgia Winson. Correspondence concerning this article should be addressed to G. M. Redding, Department of Psychology, Illinois State University, Campus Box 4620, Normal, IL 61790-4620 (e-mail: gredding@ilstu.edu).

REFERENCES

American Psychological Association (1992). Ethical principles of psychologists and code of conduct. *American Psychologist*, **47**, 1597-1611.

Barrow, H. G., & Tenenbaum, J. M. (1981). Interpreting line drawings as three-dimensional surfaces. *Artificial Intelligence*, **17**, 75-116.

Biederman, I. (1987). Recognition by components: A theory of human image understanding. *Psychological Review*, **94**, 115-147.

Biederman, I. (1995). Visual object recognition. In S. M. Kosslyn & D. N. Osherson (Eds.), *Visual cognition: An invitation to cognitive science* (2nd ed., Vol. 2, pp. 121-165). Cambridge, MA: MIT Press.

Biederman, I., & Cooper, E. E. (1992). Size invariance in visual object priming. *Journal of Experimental Psychology: Human Perception & Performance*, **18**, 121-133.

Biederman, I., & Gerhardstein, P. C. (1993). Recognizing depth-rotated objects: Evidence and conditions for three-dimensional viewpoint invariance. *Journal of Experimental Psychology: Human Perception & Performance*, **19**, 1162-1182.

Binet, A. (1895). La mesure des illusions visuelles chez les enfants. *Revue Philosophique*, **40**, 11-25.

Binford, T. O. (1981). Inferring surfaces from images. *Artificial Intelligence*, **17**, 205-244.

Christie, P. (1975). Asymmetry in the Müller-Lyer illusion: Artifact or genuine effect? *Perception*, **4**, 453-457.

Clowes, M. (1971). On seeing things. *Artificial Intelligence*, **2**, 79-116.

Cohen, J., MacWhinney, B., Flatt, H., & Provost, J. (1993). PsyScope: An interactive graphic system for designing and controlling experiments in the psychology laboratory using Macintosh computers. *Behavior Research Methods, Instruments, & Computers*, **25**, 257-271.

Coren, S., & Girgus, J. S. (1978a). *Seeing is deceiving: The psychology of visual illusions*. Hillsdale, NJ: Erlbaum.

Coren, S., & Girgus, J. S. (1978b). Visual illusions. In R. Held, H. Leibowitz, & H. L. Teuber (Eds.), *Handbook of sensory psychology* (Vol. 8, pp. 549-568). Berlin: Springer.

Day, R. H. (1972). Visual spatial illusions: A general explanation. *Science*, **175**, 1335-1340.

Day, R. H., & Dickinson, R. G. (1976). Apparent lengths of the arms of the acute and obtuse angles, and the components of the Müller-Lyer illusion. *Australian Journal of Psychology*, **28**, 137-148.

DeLucia, P. R., & Hochberg, J. (1991). Geometrical illusions in solid objects under ordinary viewing conditions. *Perception & Psychophysics*, **50**, 547-554.

Erlebacher, A., & Sekuler, R. (1974). Perceived length depends on exposure duration: Straight lines and Müller-Lyer stimuli. *Journal of Experimental Psychology*, **103**, 724-728.

Farber, J., & Rosinski, R. R. (1978). Geometric transformations of pictured space. *Perception*, **7**, 269-282.

Freeman, H. (1986). Computer graphics. In K. R. Boff, L. Kaufman, & J. P. Thomas (Eds.), *Handbook of perception and human performance: Vol. 1. Sensory processes and perception* (pp. 3.1-3.42). New York: Wiley.

Gauld, A. (1975). A note on inappropriate constancy-scaling and the Müller-Lyer illusion. *British Journal of Psychology*, **66**, 307-309.

Gibson, J. J. (1966). *The senses considered as perceptual systems*. Boston: Houghton Mifflin.

Gillam, B. (1978). A constancy-scaling theory of the Müller-Lyer illusion. In J. P. Sutcliffe (Ed.), *Conceptual analysis and method in psychology: Essays in honour of W. M. O'Neil* (pp. 57-70). Sydney: Sydney University Press.

Gillam, B. (1980). Geometrical illusions. *Scientific American*, **242**, 102-111.

Gillam, B. (1998). Illusions at century's end. In J. Hochberg (Ed.), *Perception and cognition at century's end* (pp. 95-136). New York: Academic Press.

Girgus, J. S., & Coren, S. (1982). Assimilation and contrast illusions: Differences in plasticity. *Perception & Psychophysics*, **32**, 555-561.

Gregory, R. L. (1963). Distortion of visual space as inappropriate constancy scaling. *Nature*, **199**, 678-680.

Gregory, R. L. (1965). Reply to Humphrey and Morgan. *Nature*, **206**, 745-746.

Gregory, R. L. (1967). Comments on the inappropriate constancy scaling theory of the illusions and its implications. *Quarterly Journal of Experimental Psychology*, **19**, 219-223.

Gregory, R. L. (1968). Perceptual illusions and brain models. *Proceedings of the Royal Society B*, **171**, 279-296.

Gregory, R. L. (1974). *Concepts and mechanisms of perception*. London: Duckworth.

Gregory, R. L., & Harris, J. P. (1975). Illusion-destruction by appropriate scaling. *Perception*, **4**, 203-220.

Haesen, W. (1974). An examination of R. L. Gregory's inappropriate constancy scaling theory of geometrical optical illusions. *Psychologica Belgica*, **14**, 239-259.

Heymans, G. (1896). Quantitative Untersuchungen über das "optische Paradoxen." *Zeitschrift für Psychologie*, **9**, 221-225.

Humphrey, N. K., & Morgan, M. J. (1965). Constancy and the geometric illusions. *Nature*, **206**, 744-745.

Ittelson, W. H. (1996). Visual perception of markings. *Psychonomic Bulletin & Review*, **3**, 171-187.

Jordan, K., & English, P. W. (1989). Simultaneous sampling and length contrast. *Perception & Psychophysics*, **46**, 546-554.

Jordan, K., & Haleblian, J. (1988). Orientation specificity of length assimilation and contrast. *Perception & Psychophysics*, **43**, 446-456.

Jordan, K., & Schiano, D. J. (1986). Serial processing and the parallel lines illusion: Length contrast through relative spatial separation of contours. *Perception & Psychophysics*, **40**, 384-390.

Jordan, K., & Uhlarik, J. (1985). Assimilation and contrast of perceived length depend on temporal factors. *Perception & Psychophysics*, **37**, 447-454.

Jordan, K., & Uhlarik, J. (1986). Length contrast in the Müller-Lyer figure: Functional equivalence of temporal and spatial separation. *Perception & Psychophysics*, **39**, 267-274.

Kubovy, M. (1986). *The psychology of perspective and Renaissance art*. Cambridge: Cambridge University Press.

Malik, J. (1987). Interpreting line drawings of curved objects. *International Journal of Computer Vision*, **1**, 73-103.

Marr, D. (1982). *Vision: A computational investigation in the human representation and processing of visual information*. San Francisco: Freeman.

Morgan, M. J., Hole, G. J., & Glennerster, A. (1990). Biases and sensitivities in geometrical illusions. *Vision Research*, **30**, 1793-1810.

Mountjoy, P. T. (1966). New illusory effect of the Müller-Lyer figure. *Journal of Experimental Psychology*, **71**, 119-123.

Müller-Lyer, F. C. (1981). Optical illusions (R. H. Day & H. Knuth, Trans.). *Perception*, **10**, 131-136. (Original work published in German in 1889)

Perkins, D. N. (1972). Visual discrimination between rectangular and nonrectangular parallelepipeds. *Perception & Psychophysics*, **12**, 396-400.

Perkins, D. N. (1973). Compensating for distortion in viewing pictures obliquely. *Perception & Psychophysics*, **14**, 13-18.

Piaget, J. (1969). *The mechanisms of perception* (G. N. Seagrim, Trans.). New York: Basic Books. (Original work published in French in 1961)

Pike, A. R., & Stacey, B. G. (1968). The perception of luminous Müller-Lyer figures and its implication for the misapplied constant theory. *Life Sciences*, **7**, 355-362.

Pirenne, M. H. (1970). *Optics, painting, and photography*. Cambridge: Cambridge University Press.

Predebon, J. (1994). Illusion of length in acute- and obtuse-angle figures. *Perceptual & Motor Skills*, **78**, 259-264.

Predebon, J. (2000). Length illusions in conventional and single-wing Müller-Lyer stimuli. *Perception & Psychophysics*, **62**, 1086-1098.

Pressey, A. W. (1970). The assimilation theory applied to a modification of the Müller-Lyer illusion. *Perception & Psychophysics*, **8**, 411-412.

Pressey, A. W. (1972). The assimilation theory of geometric illusions: An additional postulate. *Perception & Psychophysics*, **11**, 28-30.

Pressey, A. W. (1974). Evidence for the role of attentive field in the perception of illusions. *Quarterly Journal of Experimental Psychology*, **26**, 464-471.

Pressey, A. W., & Pressey, C. A. (1992). Attentive fields are related to focal and contextual features: A study of Müller-Lyer distortions. *Perception & Psychophysics*, **51**, 423-436.

Redding, G. M., & Hawley, E. A. (1993). Length illusion in fractional Müller-Lyer stimuli: An object-perception approach. *Perception*, **22**, 819-828.

Redding, G. M., Winson, G. D., & Temple, R. O. (1993). The Müller-Lyer contrast illusion: A computational approach. *Perception & Psychophysics*, **54**, 527-534.

Restle, P., & Decker, J. (1977). Size of the Müller-Lyer illusion as a function of its dimensions: Theory and data. *Perception & Psychophysics*, **21**, 489-503.

Rosinski, R. R., & Farber, J. (1980). Compensation for viewing point in the perception of pictured space. In M. A. Hagen (Ed.), *The perception of pictures* (Vol. 1, pp. 137-176). New York: Academic Press.

Sedgwick, H. A. (1980). The geometry of spatial layout in pictorial representation. In M. A. Hagen (Ed.), *The perception of pictures* (Vol. 1, pp. 33-90). New York: Academic Press.

Sekuler, R., & Erlebacher, A. (1971). The two illusions of Müller-Lyer: Confusion theory reexamined. *American Journal of Psychology*, **84**, 477-486.

Shepard, R. N. (1981). Psychophysical complementarity. In M. Kubovy & J. Pomerantz (Eds.), *Perceptual organization* (pp. 279-341). Hillsdale, NJ: Erlbaum.

Shepard, R. N. (1990). *Mind sights*. New York: Freeman.

Stacey, B., & Pike, R. (1970). Apparent size, apparent depth, and the Müller-Lyer illusion. *Perception & Psychophysics*, **7**, 125-128.

Sugihara, K. (1984). An algebraic approach to shape-from-image problems. *Artificial Intelligence*, **23**, 59-95.

Waltz, D. (1975). Understanding line drawings of scenes with shadows. In P. H. Winston (Ed.), *The psychology of computer vision* (pp. 19-92). New York: McGraw-Hill.

Warren, R. M., & Bashford, J. A. (1977). Müller-Lyer illusions: Their origin in processes facilitating object recognition. *Perception*, **6**, 615-626.

Yang, T., & Kubovy, M. (1999). Weakening the robustness of perspective: Evidence for a modified theory of compensation in picture perception. *Perception & Psychophysics*, **61**, 456-467.

Yue, X., Vessel, E. A., & Biederman, I. (2007). The neural basis of scene preferences. *NeuroReport*, **18**, 525-529.

NOTES

1. The terms *linear perspective* and *natural perspective* are used generically to indicate spatial layout information depicted in drawings and imaged on the retina, respectively, not just the convergence in projection of parallel lines with increasing distance. Pirenne (1970) and Kubovy (1986) discuss the important distinctions between linear perspective and pictures versus natural perspective (retinal images) and perception.

2. Gregory supposes that the natural perspective analysis responsible for size constancy is inappropriately applied to linear perspective drawings to produce illusions. He identifies two kinds of natural perspective constancy scaling: primary and secondary. Primary constancy scaling is based directly on size "cues" present in the optic array, and secondary constancy scaling employs perceived depth to "adjust" for changes in retinal image size. Most researchers have interpreted Gregory's hypothesis in terms of secondary constancy scaling, but Gregory has stressed the central position of primary constancy scaling. Consequently, most criticisms of Gregory (e.g., Gauld, 1975; Haesen, 1974; Humphrey & Morgan, 1965; Pike & Stacey, 1968; Stacey & Pike, 1970) have missed the mark and are regarded by him as largely irrelevant (Gregory, 1974).

3. However, to account for the usual asymmetry (Heymans, 1896) of the two parts of the illusion, Gillam (1978) makes the seemingly ad hoc assumption that enlargement of the line bounded by obtuse angles is greater than reduction of the line bounded by acute angles.

4. It should be noted that the study of picture perception cannot be uncritically generalized to real-world perception (Ittelson, 1996). Nevertheless, the perception of pictures is a remarkable ability that deserves attention in its own right.

5. If the present view is correct, the common practice of manipulating particular stimulus attributes without consideration of the underlying virtual structure may produce a confusion of confounds across experimental stimuli.

(Manuscript received August 18, 2008;
revision accepted for publication February 10, 2010.)